AIP | Applied Physics Letters

Quartz-enhanced photoacoustic spectroscopy exploiting tuning fork overtone modes

A. Sampaolo, P. Patimisco, L. Dong, A. Geras, G. Scamarcio, T. Starecki, F. K. Tittel, and V. Spagnolo

Citation: Applied Physics Letters **107**, 231102 (2015); doi: 10.1063/1.4937002
View online: http://dx.doi.org/10.1063/1.4937002
View Table of Contents: http://scitation.aip.org/content/aip/journal/apl/107/23?ver=pdfcov
Published by the AIP Publishing

Quartz-enhanced photoacoustic spectroscopy exploiting tuning fork overtone modes

A. Sampaolo,[1,2] P. Patimisco,[1] L. Dong,[2] A. Geras,[2,3] G. Scamarcio,[1] T. Starecki,[2,3] F. K. Tittel,[2] and V. Spagnolo[1,a)]
[1]*Dipartimento Interateneo di Fisica, Università e Politecnico di Bari, IFN-CNR UOS Bari, via Amendola 173, 70126 Bari, Italy*
[2]*Department of Electrical and Computer Engineering, Rice University, 6100 Main Street, Houston, Texas 77005, USA*
[3]*Institute of Electronic Systems, Warsaw University of Technology, Nowowiejska 15/19, 00-665 Warsaw, Poland*

(Received 13 October 2015; accepted 22 November 2015; published online 7 December 2015)

We report on a quartz-enhanced photoacoustic sensor (QEPAS) based on a custom-made quartz tuning fork (QTF) to operate in both the fundamental and the first overtone vibrational mode resonances. The QTF fundamental mode resonance falls at ~3 kHz and the first overtone at ~18 kHz. Electrical tests showed that the first overtone provides a higher quality factor and increased piezoelectric current peak values, with respect to the fundamental flexural mode. To evaluate the QTF acousto-electric energy conversion efficiency, we operated the QEPAS in the near-IR and selected water vapor as the target gas. The first overtone resonance provides a QEPAS signal-to-noise ratio ~5 times greater with respect to that measured for the fundamental mode. These results open the way to employing QTF overtone vibrational modes for QEPAS based trace gas sensing. © *2015 AIP Publishing LLC*. [http://dx.doi.org/10.1063/1.4937002]

Quartz tuning forks (QTFs) have been successfully employed as piezoelectric optoacoustic transducers in quartz-enhanced photoacoustic spectroscopic sensor (QEPAS) systems for sensitive and selective gas sensing applications.[1,2] The target gas selectively absorbs modulated laser light focused between the QTF prongs and generates acoustic waves by non-radiative energy relaxation processes. The laser modulation frequency f is set at one of the QTF resonance frequencies or at related sub-harmonics.[1] The QTF converts the acoustic waves into an electrical signal that is proportional to the gas target concentration. Non-radiative gas relaxation processes include the collision-induced energy transfer from vibrational or rotational states to translational states, with time constants depending on the specific gas carrier (typically either air or N_2) and intermolecular interactions. Time constants τ_T are in the μs range.[3] To ensure that the energy transfer follows efficiently the fast modulation f of the incident laser radiation, it is necessary to satisfy the condition $f \ll 1/2\pi\tau_T$.[4] Most QEPAS reported in the literature use standard QTFs characterized by a small volume (prong length L = 3.0 mm, thickness T = 0.35 mm, and a typical crystal width w = 0.34 mm) with a prong spacing of 300 μm. Commercial QTFs are characterized by a fundamental in-plane flexural mode with resonance frequency at ~32.76 kHz. Higher order resonances of standard QTFs cannot be implemented in a QEPAS based sensor system, since they would occur at frequencies higher than 190 kHz,[5] and thus not fulfilling the $f \ll 1/2\pi\tau_T$ condition. For gases with slow energy relaxation rates (such as CO, CO_2, and NO) the energy transfer does not efficiently follow the laser modulation at 32 kHz.[6,7] Hence, relaxation promoters (typically H_2O or SF_6) are added to the gas sample mixture in order to increase the energy relaxation process. Using this approach, enhancements of nearly 2 orders of magnitude in QEPAS signal have been reported.[1,7] However, this requires accurate measurements of the promoter concentration and additional sensor calibrations. One way to circumvent this limitation is to reduce the QTF fundamental frequency, down to a few kHz, but this leads to a decrease of the resonance quality (Q)-factor,[8] so that a trade-off optimization of the above parameters must be found. Furthermore, lowering the fundamental resonance frequency reduces also the overtone frequencies, in order to satisfy the $f \ll 1/2\pi\tau_T$ requirement. These observations led the way to an investigation of QTF overtone flexural modes for QEPAS trace gas sensing.

In this letter, we report the characterization and performance of a QTF designed to provide a fundamental resonance frequency of a few kHz. This QTF was used in a QEPAS based sensor system operating in the near-IR spectral range. The selected target gas was water vapor and allowed a comparison of the QEPAS signal using both the fundamental and the first overtone QTF flexural modes.

A QTF prong can be modeled as a single cantilever, neglecting the coupling with the other prong. The resonant frequencies f_n in vacuum of a QTF in-plane flexural mode can be related to its geometrical parameters and quartz properties by the following relation:[9]

$$f_n = \frac{\pi T}{8\sqrt{12}L^2}\sqrt{\frac{E}{\rho}}n^2, \quad (1)$$

where ρ is the density of quartz, E is the quartz Young's modulus, $n = 1.194$ for the lowest flexural mode of oscillation (fundamental mode), and $n = 2.988$ for the first overtone mode. L is the prong length and T its width, as schematically depicted in Fig. 1(a). In terms of the Q-factor, two main loss

a)Author to whom correspondence should be addressed. Electronic mail: vincenzoluigi.spagnolo@poliba.it

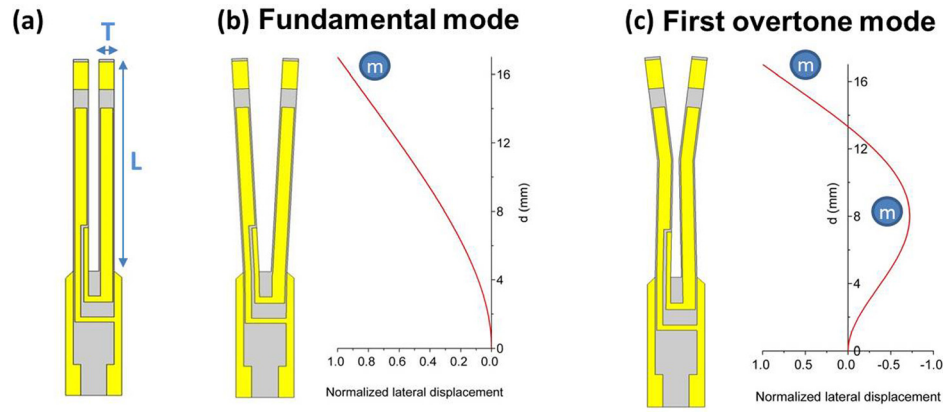

FIG. 1. (a) Schematic of the custom QTF employed in this work. $L = 17$ mm and $T = 1$ mm. (b) Lateral displacement of the prongs for the QTF fundamental flexural mode, calculated as a function of the distance from the support, d and normalized with respect to the maximum value occurring at $d = 17$ mm. (c) Normalized lateral displacement for the QTF first overtone mode, calculated as a function of d and normalized with respect to the maximum value occurring at $d = 17$ mm. Blue circles represent the point-mass subsystems. Vibration profiles of both QTF prongs are calculated using Comsol Multiphysics software (module used: solid mechanics; boundary conditions: fixed QTF support; excitations conditions: lateral boundary load on the QTF prongs top). Illustrations representing the deformation of the QTF prongs are shown in panels (b) and (c).

mechanisms, extrinsic and intrinsic, contribute to its determination. The extrinsic losses are due to interactions with the surrounding medium. The intrinsic losses include support losses (localized in the junction area between prongs and their support base), surface, volume, and thermo-elastic losses. The influence of these contributions depends on the vibrational dynamics of the selected resonance mode, since each vibrational mode is characterized by different distributions of its effective mass.[10] The fundamental in-plane flexural mode can be represented by a single point-mass on the prong tip. The support losses can be neglected and the overall Q-factor can be related to the QTF geometrical parameters by $Q \sim wT/L$.[8] The nth-overtone can be considered as a system of n-coupled point-masses subsystems, each located at an antinode and the Q-factor is mostly determined by the support losses. In fact, the overtone mode shape presents a uniform distribution of point-masses along the prong, resulting in a high stress on the QTF support. Hence, for the overtone modes, we can assume that $Q \sim Q_{supp}$ (where Q_{supp} is the inverse of support losses). For a single cantilever beam, $Q_{supp} \sim (1/n^2)(L/T)^3$ and we can assume a similar dependence for the QTF prongs.[11] Thus, even if the support losses increase with the mode number, it is possible to obtain a larger Q for overtones with respect to the fundamental mode, by optimizing the QTF dimensions. However, the reduction of the thickness T is limited, since otherwise air-damping losses become dominant.[12] The calculated vibration profiles of the QTF prongs, for maxima displacements conditions, are shown in Figs. 1(b) and 1(c), as a function of the distance from the junction between QTF prongs and their support base, for the fundamental and the first overtone modes, respectively. The vibrational profiles were calculated assuming standing waves propagating along the two QTF prongs.

We designed a QTF with $L = 17$ mm and $T = 1$ mm in order to reduce the fundamental resonance frequency f_0 by at least 1 order of magnitude with respect to the standard QTF. The prong spacing was set to 700 μm. Using Eq. (1), we calculated a resonance frequency of the fundamental flexural mode of $f_0 = 2913.42$ Hz and the first overtone mode at $f_1 = 18245.50$ Hz. Electro-elastic QTF characterizations showed that these prongs dimensions provide a high Q-factor for the first overtone flexural mode[8] and thus good performance in terms of the QEPAS signal is to be expected.[13] The custom QTF was realized by starting from a Z-cut quartz crystal plate, with a width $w = 250$ μm and a cutting angle of 2° with respect to the crystallographic X-axis, by using standard photolithographic techniques and chemical etching.[14] Electrodes of opposite polarities are deposited on adjacent sides of the QTF prongs (in a quadrupole configuration) to collect the electrical charge, employing a gold pattern similar to that used for standard QTFs. Two pins were attached on the base of the QTF for electrical connection. The QTF was fixed to a holder structure and mounted in a cell containing standard air. The gas pressure was set to 80 Torr. A waveform generator provides a sinusoidal excitation voltage to the QTF at a preset level of $V = 3.5$ mV. A current-to-voltage converter using a custom-made transimpedance amplifier with a feedback resistor of $R_F = 10$ MΩ generates a voltage signal measured by a lock-in amplifier (Stanford Research Model SR830). The obtained resonance frequencies f_n for the fundamental and the first overtone modes of the QTF, the related current peak values $I_{M,n}$, and the profile full-width at half-maximum value, Δf_n, are reported in Table I, together with the associated electrical resistance $R_n = V/I_{M,n}$ and the quality factor $Q_n = f_n/\Delta f_n$.

A very good agreement between experimental and theoretical f_n values was obtained. The small discrepancies (<3%) are mostly due to a damping gas effect, additional weight of

TABLE I. Investigated QTF parameters measured for both the fundamental and the first overtone flexural modes: resonance frequencies f_n, full width at half-maximum values Δf_n of the QTF resonance curves, quality factors Q_n, maximum current values IM,n, and electrical resistances R_n.

	Fundamental mode, n = 0	First overtone mode, n = 1
f_n (Hz)	2879.55	17788.95
Δf_n (Hz)	0.238	0.567
Q_n	12098.97	31373.81
$I_{M,n}$ (nA)	9.28	49.22
R_n (kΩ)	373.50	70.40

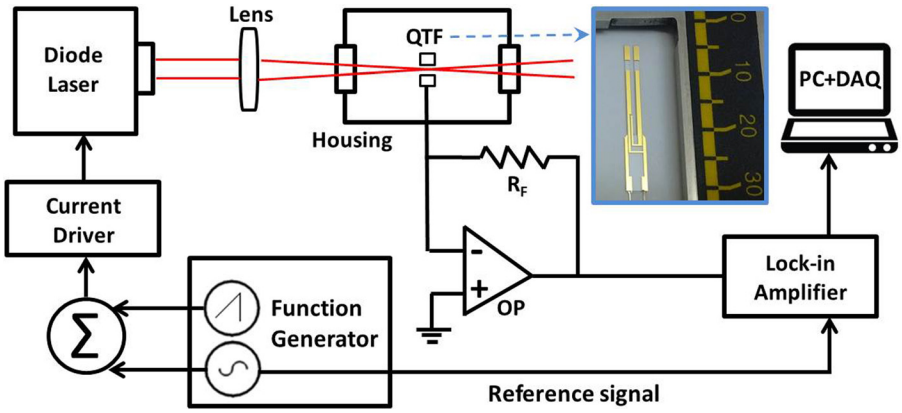

FIG. 2. Schematic of the QEPAS trace gas sensor using a diode laser as the excitation source and the investigated custom QTF. A photograph of the QTF is also shown. OP: Operational Amplifier. R_F: Feedback Resistance. PC: Personal Computer. DAQ: Data Acquisition Card.

the electrode gold layers, and slight deviations in the geometry between the modeled and the actual QTFs. The data in Table I show that the first overtone mode is characterized by a ~2.6 times higher Q-factor and a ~5.3 larger piezoelectric peak current signal, with respect to the fundamental mode. A high Q-factor and electrical conductance provide a high QEPAS signal,[4,8] which implies that the first overtone flexural mode should offer an improved performance in terms of trace gas sensing applications. To verify this assumption, we implemented the custom QTF in the QEPAS setup, as depicted in Fig. 2.

We selected water vapor as the target gas, since it is a fast relaxing molecule[15] and the excess energy transfer easily follows the laser modulation for both QTF flexural modes, which allows their comparison in terms of the QEPAS signal. The selected water line falls at 7299.43 cm^{-1} and has a line-strength of 1.01×10^{-20} cm/mol, according to the Hitran database.[16] The light source is a single-mode, continuous wave diode laser emitting at 1.37 μm, operated by means of a current driver. The laser power was fixed at 10 mW. The laser beam was then focused between the prongs of the QTF by using a lens with a focal length of 40 mm. The housing accommodating the QTF was filled with air samples containing a fixed concentration of 1.7% of water using a Nafion humidifier, at different pressure values. A wavelength modulation approach for QEPAS detection was used by applying a sinusoidal dither at half of the resonant frequency to the diode laser current by means of a function generator. The QTF response was detected at the resonant frequency by means of a lock-in amplifier. QEPAS spectral measurements were performed by slowly scanning the laser wavelength by means of a low-frequency (10 mHz) voltage ramp applied to the diode laser current driver. The acoustic source must be located at the antinodes points of the vibration mode profile, where a maximum vibration amplitude is allowed. These points were identified by scanning the laser focusing position along the QTF symmetry axis in steps down to 250 μm and measuring the associated QEPAS signal, as shown in Fig. 3.

The diode laser beam positions at the maximum QEPAS signal occur at $d = 15$ mm and $d = 7.5$ mm from the bottom of the prongs for the fundamental and overtone modes, respectively. The discrepancy with the calculated vibrational profiles results from the spherical symmetry of the exciting acoustic wave. The closer to the prong top is the vertical position of the acoustic source, the larger is the fraction of the pressure wave not hitting the prong. This downshifts the optimum vertical position of the laser spot for the first flexural mode[1] and favors the antinode at $d = 8$ mm for the first overtone mode. The increase in signal observed for the fundamental flexural mode at low d values is a known phenomenon due to an optothermal effect generated by excited molecules diffusing from the laser beam area to the QTF surface. This produces a periodic local heating of the quartz crystal and a subsequent thermal expansion of the heated region, forcing a resonant vibration of the QTF.[17] However, under these conditions, the noise signal considerably increases, leading to poor signal-to-noise levels.

Optimization of the QEPAS detection performance in terms of signal-to-noise ratio requires that both the gas pressure and the wavelength modulation depth must be appropriately chosen. The gas pressure influences the QEPAS signal in the following way: if pressure increases, the Q-factor decreases, while the energy relaxation efficiency is higher and vice-versa. Thus, a compromise must be found in order to achieve efficient sound production. In our case, since for water vapor both the investigated QTF resonance frequencies satisfy the condition $f \ll 1/2\pi\tau_T$, negligible differences in the optimal gas pressure values are to be expected. The QEPAS peak signal for both flexural modes were recorded as a function of the gas pressure in the range of 10–400 Torr and for both modes the QEPAS signal exhibits its maximum value at

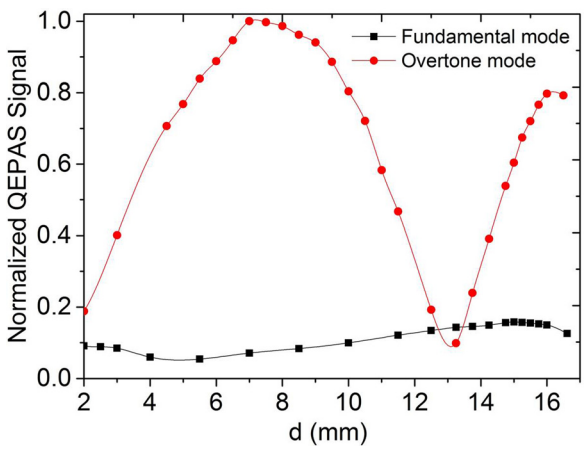

FIG. 3. Normalized QEPAS signal as a function of the beam distance from the QTF support measured for the fundamental and the first overtone modes at a pressure of 75 Torr. The laser beam position was scanned along the symmetry axis of the QTF. All data are normalized to the QEPAS highest signal, measured for the first overtone mode at $d = 7.5$ mm.

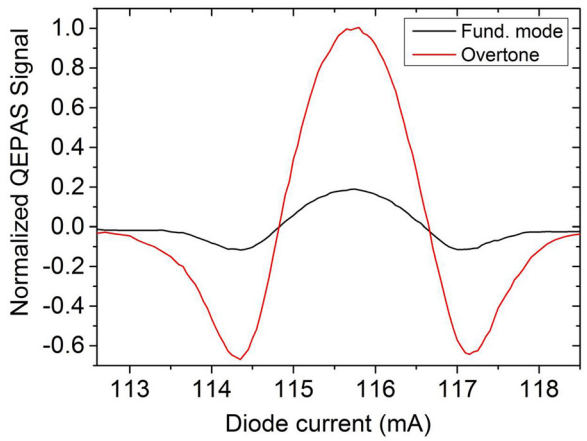

FIG. 4. QEPAS spectral scans of a gas mixture containing air with a 1.7% water concentration at a pressure of 75 Torr for the fundamental mode (black solid line) and for the first overtone mode (red solid line), acquired at the optimum laser modulation depth and focusing point conditions. Both scans were recorded with a 100 ms lock-in integration time and normalized to the overtone peak value. The overtone peak signal corresponds to 2.65 mV.

the same pressure of 75 Torr. Investigations of the diode laser modulation depths on the QEPAS signal reveal that the values maximizing the QEPAS signal occur at 5 mA for both the fundamental and overtone modes, corresponding to a frequency modulation of $0.05\,cm^{-1}$. For the optimum operating conditions, the largest QEPAS signal (2.65 mV) was observed for the first overtone mode. The spectral scans obtained for each vibrational mode are shown in Fig. 4, normalized to the overtone peak value.

The two QEPAS spectra show the same noise level ($\sim 30\,\mu V$), while the peak value measured for the first overtone mode is $\sim$5.3 times higher than that obtained using the fundamental mode. These results clearly demonstrate that the investigated QTF operating in the first overtone flexural mode is advantageous in terms of the QEPAS signal-to-noise ratio. Furthermore, by operating at a QTF frequency of $\sim$18 kHz allows the use of an acoustic micro-resonator tube system (as typically employed in standard QEPAS to confine the sound wave between the QTF prongs) to further enhance the QEPAS signal-to-noise ratio.[1] This approach is not feasible for the fundamental mode at $\sim$3 kHz, since it would require tube lengths of several centimeters, making the optical alignment impractical.[18] Furthermore, the employed QTF gold-contact pattern maximizes the electrical-mechanical coupling for the fundamental vibrational mode. Instead, the first flexural overtone mode is characterized by two nodal points of motion of the prongs (see Fig. 1(c)), and an optimal charge collection requires polarity changes of the electrodes along the prongs, which can only be realized by an octupole gold pattern configuration. An additional enhancement of the QEPAS signal-to-noise ratio is expected upon realizing such a QTF contact design.

The authors from the Dipartimento Interateneo di Fisica di Bari acknowledge the financial support from Italian Research Projects PON02 00675, PON02 00576, and PON03-Sistema. A. Geras acknowledges support from the Kosciuszko Foundation. Frank K. Tittel acknowledges support from the National Science Foundation (NSF) ERC MIRTHE award and the Robert Welch Foundation (Grant No. R4925S).

[1]P. Patimisco, G. Scamarcio, F. K. Tittel, and V. Spagnolo, Sensors **14**, 6165 (2014).
[2]A. A. Kosterev, F. K. Tittel, D. V. Serebryakov, A. L. Malinovsky, and I. V. Morozov, Rev. Sci. Instrum. **76**, 043105 (2005).
[3]W. H. Flygare, Acc. Chem. Res. **1**, 121 (1968).
[4]A. A. Kosterev, Y. A. Bakhirkin, and F. K. Tittel, Appl. Phys. B **80**, 133 (2005).
[5]J. M. Friedt and É. Carry, Am. J. Phys. **75**, 415 (2007).
[6]V. Spagnolo, A. A. Kosterev, L. Dong, R. Lewicki, and F. K. Tittel, Appl. Phys. B **100**, 125 (2010).
[7]L. Dong, V. Spagnolo, R. Lewicki, and F. K. Tittel, Opt. Express **19**, 24037 (2011).
[8]P. Patimisco, A. Sampaolo, L. Dong, M. Giglio, G. Scamarcio, F. K. Tittel, and V. Spagnolo, "Analysis of the electro-elastic properties of custom quartz tuning forks for optoacoustic gas sensing," Sens. Actuators, B (submitted).
[9]P. Patimisco, S. Borri, A. Sampaolo, H. E. Beere, D. A. Ritchie, M. S. Vitiello, G. Scamarcio, and V. Spagnolo, Analyst **139**, 2079 (2014).
[10]R. R. Archer, N. H. Cook, S. H. Crandall, N. C. Dahl, F. A. McClintock, E. Rabinowicz, and G. S. Reichenbach, *An Introduction to the Mechanics of Solids* (McGraw-Hill, New York, 1959).
[11]Z. Hao, A. Erbil, and F. Ayazi, Sens. Actuators, A **109**, 156 (2003).
[12]H. Hosaka, K. Itao, and S. Kuroda, Sens. Actuators, A **49**, 87 (1995).
[13]A. A. Kosterev, Y. A. Bakhirkin, F. K. Tittel, S. Mcwhorter, and B. Ashcraft, Appl. Phys. B **92**, 103 (2008).
[14]S. Lee, J. Y. Lee, and T. S. Park, Mater. Corros. **52**, 712 (2001).
[15]J. Finzi, F. E. Hovis, V. N. Panfilov, P. Hess, and C. B. Moore, J. Chem. Phys. **67**, 4053 (1977).
[16]L. S. Rothman, I. E. Gordon, Y. Babikov, A. Barbe, D. Chris Benner, P. F. Bernath, M. Birk, L. Bizzocchi, V. Boudon, L. R. Brown, A. Campargue, K. Chance, E. A. Cohen, L. H. Coudert, V. M. Devi, B. J. Drouin, A. Fayt, J.-M. Flaud, R. R. Gamache, J. J. Harrison, J.-M. Hartmann, C. Hill, J. T. Hodges, D. Jacquemart, A. Jolly, J. Lamouroux, R. J. Le Roy, G. Li, D. A. Long, O. M. Lyulin, C. J. Mackie, S. T. Massie, S. Mikhailenko, H. S. P. Müller, O. V. Naumenko, A. V. Nikitin, J. Orphal, V. Perevalov, A. Perrin, E. R. Polovtseva, C. Richard, M. A. H. Smith, E. Starikova, K. Sung, S. Tashkun, J. Tennyson, G. C. Toon, V. G. Tyuterev, and G. Wagner, J. Quant. Spectros. Radiat. Transfer **130**, 4 (2013).
[17]A. A. Kosterev and J. H. Doty, Opt. Lett. **35**, 3571 (2010).
[18]L. Dong, A. A. Kosterev, D. Thomazy, and F. K. Tittel, Appl. Phys. B **100**, 627 (2010).